water

MDPI

Article

Spatio-Temporal Characteristics and Trend Prediction of Extreme Precipitation—Taking the Dongjiang River Basin as an Example

Ningning Li [1,2,3,4,*], Xiaohong Chen [1], Jing Qiu [2,3,4], Wenhui Li [5] and Bikui Zhao [2,3,4]

[1] Water Resources and Environment Research Center, School of Civil Engineering, Sun Yat-Sen University, Guangzhou 510275, China
[2] Guangdong Research Institute of Water Resources and Hydropower, Guangzhou 510635, China
[3] National and Local Joint Engineering Laboratory of Estuary Hydropower Technology, Guangzhou 510635, China
[4] Guangdong Water Security Collaborating Innovation Center, Guangzhou 510635, China
[5] The Key Laboratory of Virtual Geographic Environment (MOE), Nanjing Normal University, Nanjing 210023, China
* Correspondence: linn57@mail.sysu.edu.cn

Abstract: The intricate interplay between human activities and climate change has resulted in a rise in the occurrence of extreme precipitation worldwide, which has attracted extensive attention. However, there has been limited dissemination of accurate prediction of extreme precipitation based on analysis of spatio-temporal characteristics of such events. In this study, the intra-annual distribution of extreme precipitation was subjected to scrutiny via an analysis of precipitation concentration degree (PCD) and precipitation concentration period (PCP), while also investigating the spatio-temporal trends of the annual precipitation, maximum daily precipitation, maximum 5-day precipitation, and extreme precipitation (defined as daily precipitation exceeding the 99th percentile of the total precipitation). Furthermore, subsequently, conducting simulation, verification, and prediction of extreme precipitation was achieved through the application of a back-propagation artificial neural network (BP-ANN). This study employed the data of the daily precipitation in the Dongjiang River Basin from 1979 to 2022, a time period which was of sufficient length to reflect the latest changes in precipitation patterns. The results demonstrated spatio-temporal differences between precipitation levels in the upper and lower reaches of the Dongjiang River Basin, that is, the PCD of the lower reach was higher and the PCP of the lower reach came half a month later compared with the upper reach. Moreover, the extreme precipitation indices increased from northeast to southwest, with the characteristics of lower-reach precipitation being more extreme and periodic. It was predicted that the total precipitation in 2023 would decrease, while the extreme precipitation would increase. The qualification rate of forecasting extreme precipitation ranged from 27% to 72%.

Keywords: Dongjiang River Basin; extreme precipitation; precipitation concentration degree (PCD); precipitation concentration period (PCP); artificial neural network; precipitation forecast

Citation: Li, N.; Chen, X.; Qiu, J.; Li, W.; Zhao, B. Spatio-Temporal Characteristics and Trend Prediction of Extreme Precipitation—Taking the Dongjiang River Basin as an Example. *Water* **2023**, *15*, 2171. https://doi.org/10.3390/w15122171

Academic Editors: Achim A. Beylich and Roohollah Noori

Received: 17 April 2023
Revised: 26 May 2023
Accepted: 6 June 2023
Published: 8 June 2023

1. Introduction

With global climate change, the rapid development of cities, and the intensification of human activities in recent years, the occurrence of extreme weather events has become increasingly frequent in China, with floods and droughts occurring alternately [1–3]. The increasing frequency of extreme precipitation events, particularly rainstorms, poses a significant threat to water supply security, food security, and human life in water-rich regions, leading to a heightened risk of floods and presenting substantial challenges to water security in these areas [4–6].

Extreme precipitation has been widely discussed and investigated globally. Indeed, the spatio-temporal dynamics of extreme precipitation in specific regions have been analyzed

from various perspectives, including occurrence, duration, cumulative volume, intensity, frequency, and other feature indices of extreme precipitation events [7–9]. The utilization of the precipitation concentration degree (PCD) and precipitation concentration period (PCP) has become widespread in the investigation of the temporal distribution of precipitation [10,11]. Furthermore, other feature indices, such as the annual maximum precipitation, hourly heavy precipitation (20–50 mm/h), hourly extremely heavy precipitation (≥50 mm/h), daily maximum precipitation, extreme precipitation, and other indicators for 3, 5, or 7 consecutive days have also been frequently adopted to describe and analyze the spatio-temporal variation characteristics of extreme precipitation [12–14]. Based on various feature indices of extreme precipitation events, different methods, such as the Mann–Kendall test [15,16], the Student's *t* test, and the extreme value theory, have been utilized in the investigation of regional extreme precipitation characteristics [17–19]. In these studies, extreme precipitation was predicted based on evaluating its characteristics and trends from different perspectives. However, data series' lack of timeliness make them insufficient to reflect the characteristics of extreme precipitation over the past decade under climate change and human activities [20]. What is more, extensive research has been conducted to study the long-term trend of extreme precipitation in the future, which is of little significance for guiding recent water resource management. As a result, based on the analysis of spatio-temporal characteristics, the accurate forecasting of short-term trends of extreme precipitation indices can be of great significance in terms of proactive water resource management, with example being making water use plans and hydroelectric power generation plans in advance, so as to create more comprehensive benefits.

The artificial neural network (ANN) model is effective for predicting precipitation. It ignores the physical mechanisms between the prediction factors and the predicted targets, and establishes a model that is only driven by the data itself. Bodri et al. [21] trained a BP-ANN model using the actual monthly precipitation data from two Moravia meteorological stations and drew the conclusion that it was highly feasible for forecasting precipitation. André et al. [22] clarified that data-driven models did not rely on a specific study region. Vandal et al. [23] verified that different machine learning methods performed differently in predicting various precipitation indices, even though the most advanced machine learning methods could not provide direct improvements compared to simpler ones. Therefore, this prompts us to attempt to use the BP-ANN model, widely used in rainfall prediction, to predict the performance of extreme precipitation indices in 2023.

The Dongjiang River Basin in Guangdong is located at the northeastern end of the Pearl River Basin. It lies within the subtropical monsoon humid climate zone, with distinctive low- and high-precipitation seasons. Winter and spring represent the low-precipitation seasons, while summer and autumn exhibit high temperatures and significant rainfall [24,25]. The altitude was recorded as high in the northeast, while it was low in the southwest. Additionally, this geographical feature is extremely responsive to alterations in the climate [26]. The Dongjiang River Basin plays a crucial role in providing water resources to support the Guangdong–Hong Kong–Macao Greater Bay Area, which is a world-class urban agglomeration [27–29]. However, for a long period, the water projects implemented in the basin have adopted conservative scheduling and operational methods, which have resulted in limited comprehensive utilization functions. These methods are no longer compatible with the changing trends and utilization requirements of water resources [30]. Therefore, it is imperative to analyze and predict the spatio-temporal characteristics of extreme precipitation in the basin to gain thorough comprehension of precipitation patterns, as well as to maximize water resource usage. This can further offer guidance for the reasonable planning, scheduling, and utilization of water resources in the Dongjiang River Basin.

Based on the PCD, PCP, annual precipitation, maximum daily precipitation, maximum five-day precipitation, and extreme precipitation, this study quantitatively and qualitatively analyzed the intra-annual concentration, long-term trend, and spatial distribution of extreme precipitation in the Dongjiang River Basin. Grid data of daily precipitation which

were characterized by highest timeliness were employed. Moreover, an extreme precipitation indices forecasting method based on a back-propagation artificial neural network (BP-ANN) was proposed for the accurate prediction of extreme precipitation events in this basin in 2023.

2. Study Area and Data

2.1. Study Area

The Dongjiang River Basin is situated in the eastern part of China and the eastern end of the Pearl River Basin, geographically positioned between E113°52′~115°52′ and N22°38′~25°14′. The altitude of the region is high in the northeast and low in the southwest. The drainage basin has complex topographic features, including mountains, hills, river valleys, plains, and river delta network areas. The basin is located in Guangdong Province and features a drainage area of 31,840 km^2, which accounts for 90% of the entire drainage area [25]. The topography and rainfall station locations of the Dongjiang River Basin are shown in Figure 1.

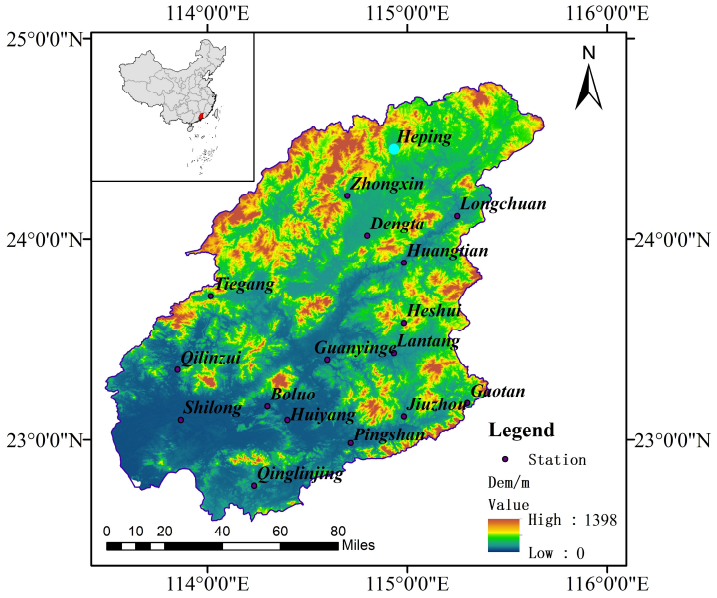

Figure 1. Geographical location and 18 meteorological stations of the Dongjiang River Basin.

The annual average precipitation level within the basin falls within 1500–2400 mm, with the potential evaporation averaging 1048 mm and the total water resources averaging 33 billion m^3 per year (1956–2016). The Dongjiang River is the primary source of fresh water for the major cities of the Pearl River delta (e.g., Hong Kong, Guangzhou, Shenzhen, and Dongguan). The quantity and quality of water available in this region are considered to be major issues for the Dongjiang River Basin [27]. Therefore, the Dongjiang River Basin plays a pivotal role in the province's politics, society, and economy. Due to human activities, topographic features, and climate change, there are significant differences in precipitation patterns between upper and lower reaches of the basin. To facilitate analysis, the Dongjiang River Basin was divided into upper and lower reaches, with the boundary located at the Qiuxiang River estuary.

2.2. Data

The daily precipitation time series data of the Dongjiang River Basin from 1979 to 2022 were derived from the CPC Global Unified Gauge-Based Analysis of Daily Precipitation dataset of National Oceanic and Atmospheric Administration (NOAA) (https://www.noaa.gov/ (accessed on 30 March 2023), with a resolution of 0.5 degrees latitude × 0.5 degrees longitude. All spatial data were standardized to a common geographic coordinate system and projection. The missing data were substituted with the average precipitation of adjacent

grids. By utilizing the kriging method for spatial interpolation of grid data, the data reflecting the spatio-temporal characteristics of extreme precipitation in the upper and lower reaches were collected.

A set of extreme climate indices was proposed in climate change monitoring conferences from 1998 to 2001 by the World Meteorological Organization (WMO) which has become the benchmark for climate change research. The set includes 11 core indices on extreme precipitation, which are calculated from daily precipitation data and have the properties of weak extremes, low noise, and strong significance [31]. In this study, four indices reflecting the intensity of extreme precipitation (annual precipitation, extreme precipitation, daily maximum precipitation, and maximum five-day precipitation) were employed for the investigation of extreme precipitation in the Dongjiang River Basin, as shown in Table 1.

Table 1. Extreme precipitation indices (mm).

Indicator	Full Name	Meaning
PRCPTOT	annual precipitation	precipitation daily cumulative amount $\geq$ 1 mm
R99p	extreme precipitation	sum of daily precipitation > 99% percentile
RX1day	daily maximum precipitation	annual maximum daily precipitation
RX5day	maximum five-day precipitation	annual maximum five-day precipitation

3. Methods

3.1. Method for Prediction of Intra-Annual Trend

The PCD and PCP are metrics that can be used to calculate and analyze the intra-annual distribution of precipitation [10]. A year, comprising 365 days (or 366 days in leap years), was treated as a circle and divided into corresponding angles for each day as the vector directions (see Figure 2). The daily precipitation was considered as the magnitude of the vector, and the daily precipitation for a year was summed according to vector addition principles. Therefore, each daily precipitation value was aggregated into a vector, where the ratio of its modulus to the annual precipitation amount was termed the PCD, and its direction (angle) was termed the PCP.

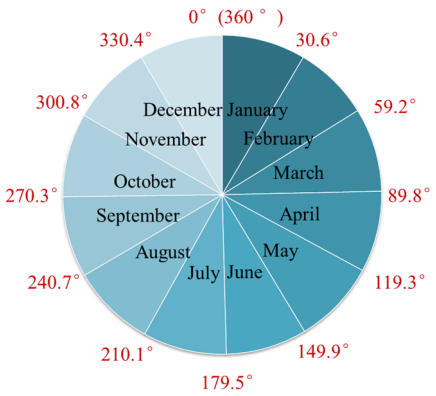

Figure 2. Relationship between 12 months in a year and the angle of PCP (taking non-leap year as an example).

According to the calculation principle, the PCD is an effective measure of the heterogeneous intra-year distribution of precipitation. When the precipitation is entirely concentrated on a certain day, the ratio of the modulus of the composite vector to the total annual runoff is equivalent to 1, which is the maximum possible value of the PCD. Conversely, if the daily precipitation is uniform, the PCD is 0, indicating that the yearly runoff is uniformly distributed throughout each day of the year. The PCP reflects the time span when the maximum rainfall occurs in a year.

3.2. Method for Prediction of Inter-Year Trend

The Mann–Kendall Test and wavelet analysis were employed to investigate the trends, changes, and periodicities of extreme precipitation indices.

The Mann–Kendall Test, denoted as the MK test, is a non-parametric test (no-distribution test). It does not rely on distribution assumptions and is free from interference by abnormalities. Hence, it has been extensively employed to analyze time series trends and breakpoints of precipitation, runoff, air temperature, and water quality [32,33].

Wavelet analysis involves approximating a certain signal or function through the usage of a series of wavelet functions, which correspond to different frequencies (scales). This method allows for the effective extraction of periodic changes in the time series across various scales. Therefore, wavelet analysis is commonly used to investigate the periodic variations present in time series.

In this study, the Morlet continuous complex wavelet in the one-dimensional (1D) continuous wavelet was adopted to conduct periodicity analysis of the precipitation sequence. The wavelet coefficient allows for the analysis of periodic characteristics and the strength of the time series at various time scales. The wavelet variance, obtained by the integration of the squared wavelet coefficient across the b domain, is utilized to analyze the fluctuation energy across various cycle scales. By identifying the peak values, the main change cycles of the time series can be determined [34].

3.3. BP-ANN

A BP-ANN simulates the functioning of neural networks in the human brain. In 1986, a research team led by Rumelhart and Hinton [35] published research results on BP-ANNs in *Nature*, and they have been widely applied in learning, association, memory, and pattern recognition. A BP-ANN is a multi-layer feed-forward network trained by the error back-propagation algorithm [36]. It consists of an input layer, a hidden layer, and an output layer, as shown in Figure 3.

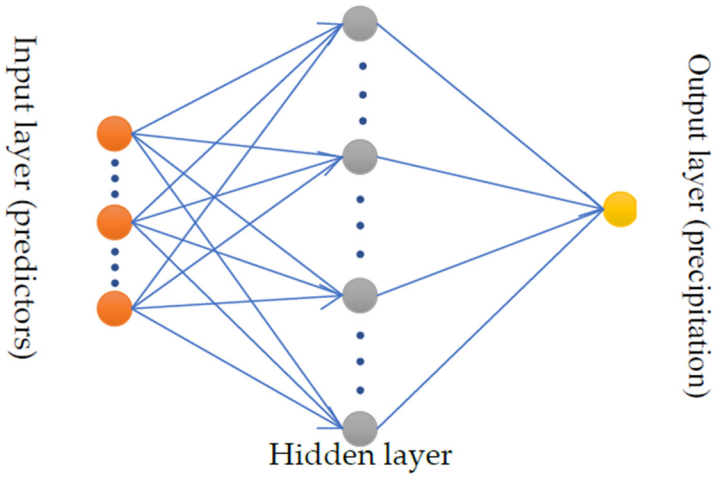

Figure 3. Precipitation forecast by BP-ANN.

A BP-ANN has the ability to store the learned input–output mapping relationship without prior knowledge of the functional relationship between them. By training the model through the application of historical precipitation data, the mapping relationship between the prediction factor and the forecast runoff process can be established and recorded. The trained model can be used to forecast future precipitation processes.

To predict the characteristics of short-term extreme precipitation, early-stage extreme precipitation index sequences of periods $t-1$, $t-2$, and $t-3$ were used as the input layer of the BP-ANN model, and early-stage extreme precipitation index sequences of period t were employed as the output layer. The extreme precipitation data of the Dongjiang River Basin during 1979–2022 were utilized for the training and testing of the prediction

model. The hyperbolic tangent function was adopted as the neuron transfer function. The neuron quantity in the hidden layer was set to be 10, and the training iteration count was set to be 10,000. Typically, extreme precipitation prediction is challenging, and the overall qualification rate has been low. Additionally, replicates were conducted to guarantee the effectiveness of analysis. Therefore, predicted values with a qualification rate exceeding 20% for 100 tests were collected. The collected values were statistically analyzed for potential trends with high, medium, or low probabilities.

$$QR = \frac{n}{N} \times 100\% \quad (1)$$

where N represents the length of the sequence and n represents the number of qualified predictions.

4. Analysis of Spatio-Temporal Variation Characteristics

4.1. Trends of Intra-Annual Distribution Indices

According to the daily precipitation process data from 1979 to 2022, the PCD and PCP of the upper and lower reaches of the Dongjiang River Basin in these years were calculated, which are respectively reflected by the polar diameter and polar angle shown in Figure 4. Overall, the upper-reach precipitation of the Dongjiang River Basin was mainly concentrated in the polar angle of 100~210°, with a mean of 159°, while the lower-reach precipitation was concentrated in 120~210°, with a mean of 175°, which indicated that upper-reach precipitation mostly occurred in June, while lower-reach precipitation mostly occurred in July. The polar diameter distribution of the upper reach ranged from 0.2 to 0.6, with a mean of 0.43, while the distribution of lower reach ranged from 0.3 to 0.65, with a mean of 0.48. This suggested that the intra-annual PCD of the lower reach was higher, and the possibility of extreme precipitation was also higher than that of the upper reach.

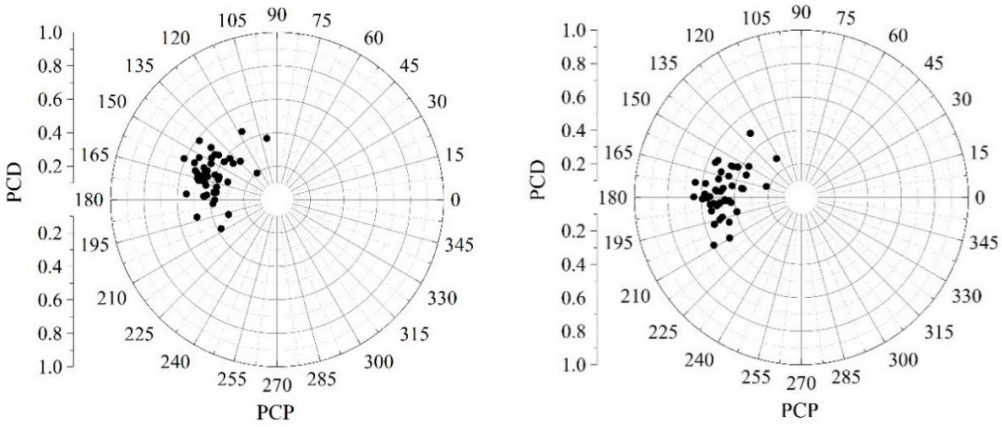

Figure 4. Polar coordinates representing the intra-annual concentration of precipitation: (**a**) upper reach; (**b**) lower reach.

By using the MK test, both the regularity and features of the inter-annual variation of the PCD and PCP were identified (Figure 5). The Z values of the PCD and PCP in the upper and lower reaches of the Dongjiang River Basin were all greater than 0, which indicated an enhancement in the PCD of the entire basin and a delay in the occurrence time of the main precipitation. This trend was more obvious in the upper reach than in the lower reach, but it was not significantly different. Especially, the UF line of the PCD values of the upper and lower reaches exceeded the significance test line, suggesting a significant increase from 2005 to 2010 with a 95% CI. Additionally, 1992 was a common mutation point where the UB and UF intersected, indicating that there was a sudden increase after 1992.

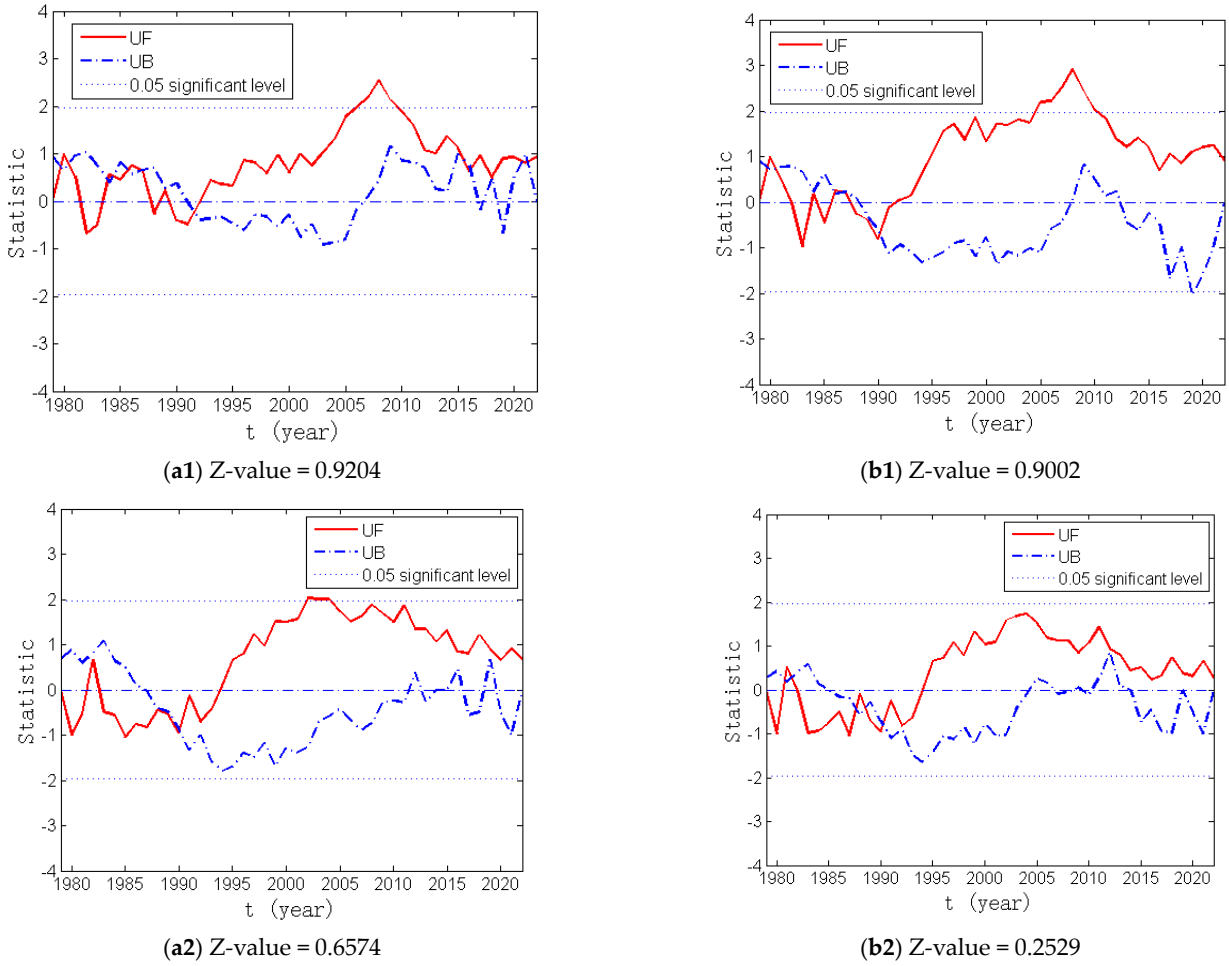

(**a1**) Z-value = 0.9204

(**b1**) Z-value = 0.9002

(**a2**) Z-value = 0.6574

(**b2**) Z-value = 0.2529

Figure 5. The MK test results of the time series of the PCD and PCP: (**a1**) {upper reach, PCD}; (**a2**) {upper reach, PCP}; (**b1**) {lower reach, PCD}; (**b2**) {lower reach, PCP}. The y-axis represents the statistics of the UF and UB.

4.2. Trends of Extreme Precipitation Indices

Figure 6 illustrates the spatial distribution of the averages of the four extreme precipitation indices of the Dongjiang River over the past 40 years. The Dongjiang River Basin exhibited multi-year means of 1700~2200 mm, 150~220 mm, 45~70 mm, and 120~200 mm for the PRCPTOT, R99p, RX1day, and RX5day, respectively. Furthermore, the lower reach experienced values 1.3, 1.5, 1.6, and 1.7 times higher, respectively, than those of the upper reach, showing an obvious increasing trend from north to south.

Figure 7 summarizes the percentages of three extreme precipitation indices of the annual precipitation. As observed, the percentages of the RX1day, RX5day, and R99p were 5%, 10%, and 15%, respectively. In addition, the proportion of extreme precipitation in the lower reach was generally higher than that in the upper reach, indicating that the precipitation in the lower reach was more extreme. The increase in tropical cyclone intensity in the western Pacific due to global warming has led to the strengthening of extreme precipitation in the lower reach of the Dongjiang River [37]. Notably, the RX5day of the upper reach exceeded the R99p in 2005 and 2020, both of which were dry years, indicating that, in years with less precipitation, extreme precipitation may be concentrated and continuously produced by only one precipitation event. Moreover, the proportion of extreme precipitation in the whole year was higher in 1999, 2005, and 2019, and the RCD was larger in these years. This suggested that, when the proportion of extreme precipitation was high, the intra-annual PCD was more likely to be high. This indicated that the annual precipitation of the Dongjiang River Basin may be highly concentrated in several extreme

precipitation events, resulting in an uneven spatio-temporal distribution of precipitation, as well as leading to drought for most of the year. Therefore, a water storage project is required to regulate and distribute water resources spatio-temporally.

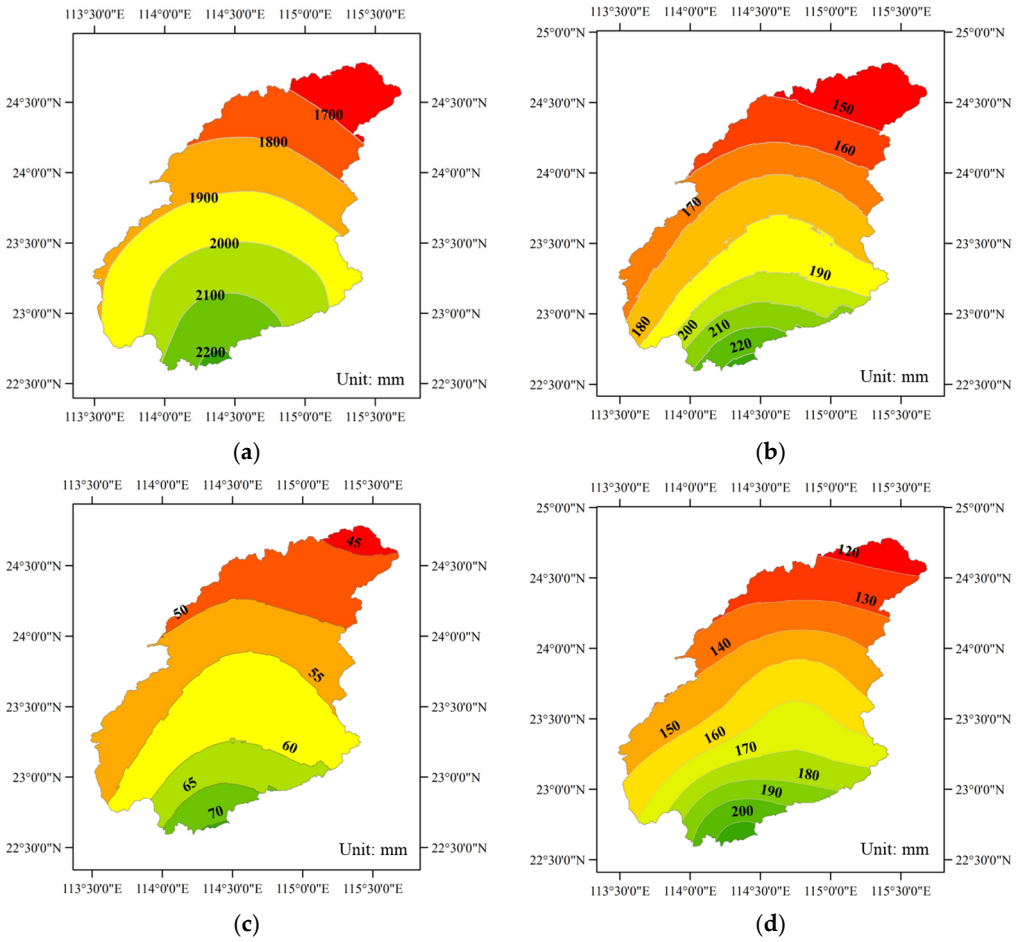

Figure 6. Spatial distribution of (**a**) PRCPTOT, (**b**) R99p, (**c**) RX1day, and (**d**) RX5day of the Dongjiang River Basin.

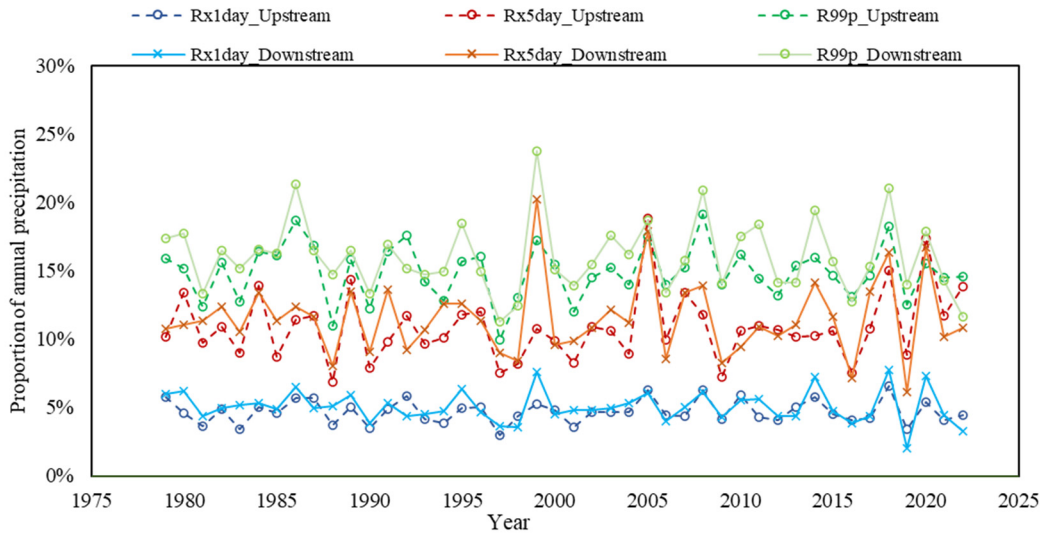

Figure 7. The proportion of extreme precipitation indices to annual precipitation.

We aimed to identify the trend of extreme precipitation in the Dongjiang River Basin and the differences between the upper and lower reaches from the time series of annual extreme precipitation indices in the period of 1979–2022. The results of the MK test in Figure 8 demonstrated that the PRCPTOT of the upper reach illustrated a downward trend, while the R99p, RX1day, and RX5day exhibited an upward trend. The PRCPTOT, R99p, RX1day, and RX5day of the lower reach all showed downward trends. Among them, the R99p and RX1day of the lower reach passed tests with a 90% CI and 95% CI, respectively, indicating a significant downward trend. This trend was followed by the PRCPTOT of the upper reach and the RX5day of the lower reach, both of which also demonstrated relatively strong downward trends. This can be attributed to the fact that the upper-middle reach of the Dongjiang River Basin is dominated by mountainous hills and valleys, where frontal rain events are prevalent, commonly occurring from April to June due to the impact of warm and humid airflow in the western Pacific Ocean. In contrast, the lower reach is dominated by plains, and the precipitation is mostly brought by a tropical cyclone, which typically occurs from July to September. Hence, the intra-annual distributions of precipitation of the upper and lower reaches of the Dongjiang River Basin differed significantly.

With the exception of the RX1day in the upper reach and the R99p of lower reach, the intersection points of the UB and UF for other indicators were between 1980 and 2005. Afterward, the statistical values' absolute values increased. We considered this point to be an abrupt point where the trend changes from increasing to declining, and the trend of change strengthened. The R99p and RX5day of the upper reach and the R99p and PRCPTOT of the lower reach had multiple intersections after 2020, mainly due to the weakening change of the trend.

Through wavelet analysis, we extracted the real part of the wavelet coefficient (Figure 9), which reflected the periodicity of the alternating abundance and dryness of the precipitation on different time scales. Red coloring indicates a positive wavelet coefficient, representing more annual precipitation, while blue coloring indicates a negative wavelet coefficient, representing less annual precipitation. The first and second principal periods are referred to as 1st-mp and 2nd-mp, respectively.

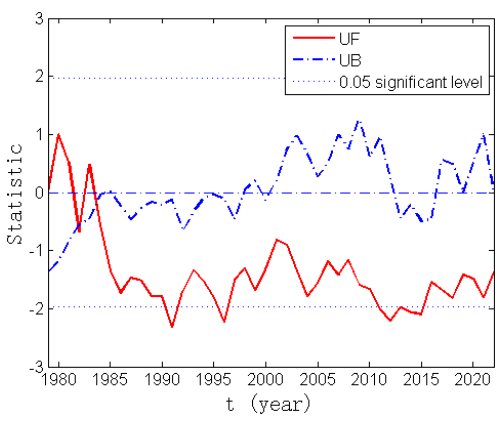

(**a1**) Z-value = −1.3654

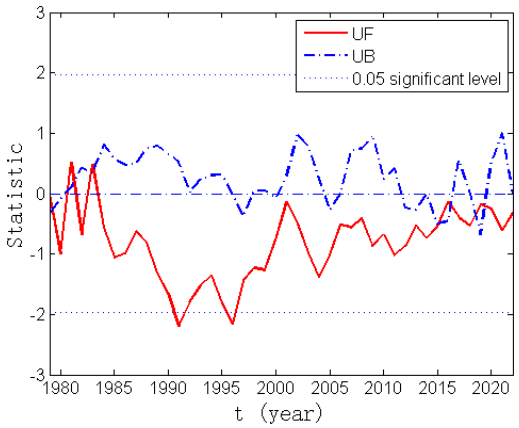

(**b1**) Z-value = −0.3135

Figure 8. *Cont.*

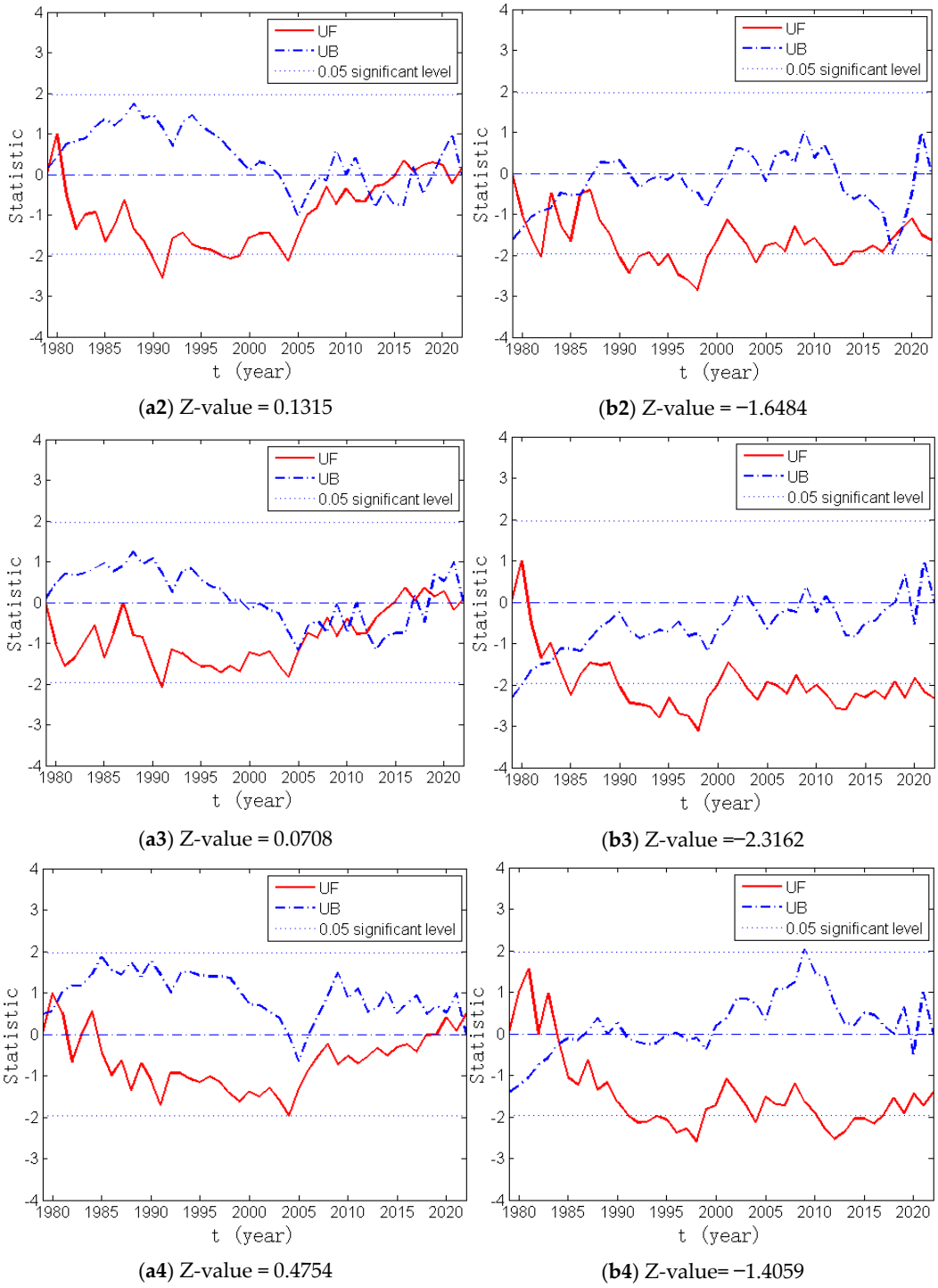

(**a2**) Z-value = 0.1315 (**b2**) Z-value = −1.6484

(**a3**) Z-value = 0.0708 (**b3**) Z-value =−2.3162

(**a4**) Z-value = 0.4754 (**b4**) Z-value= −1.4059

Figure 8. The MK test results of upper-reach extreme precipitation indices time series. (**a**) upper reach; (**b**) lower reach; (1–4) PRCPTOT, R99p, RX1day, and RX5day. The y-axis represents the statistics of the UF and UB.

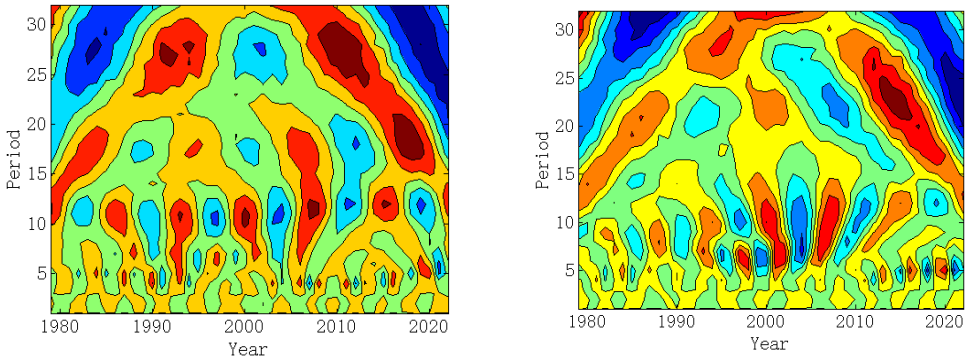

(**a1**) 1st-mp = 5, 2nd-mp = 12 (**b1**) 1st-mp = 22, 2nd-mp = 7

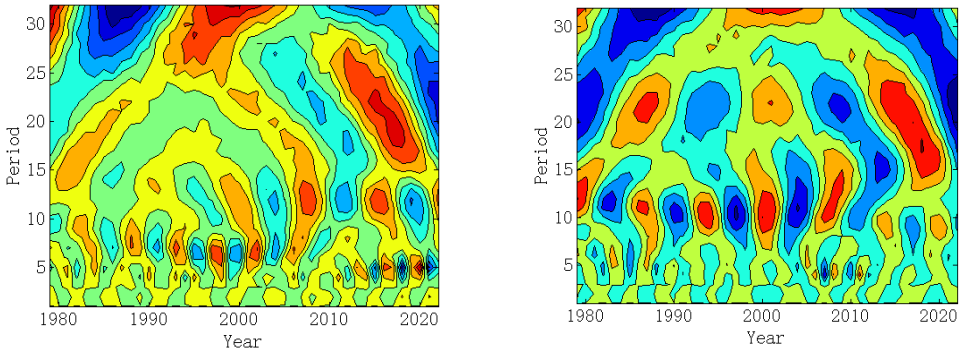

(**a2**) 1st-mp = 28, 2nd-mp = 11 (**b2**) 1st-mp = 22, 2nd-mp = 11

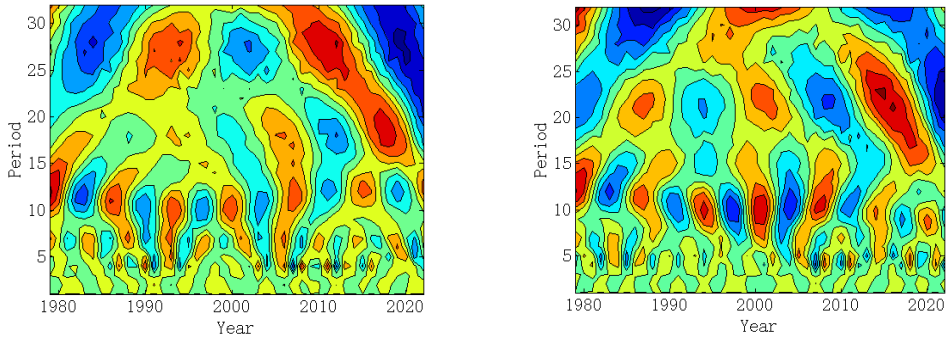

(**a3**) 1st-mp = 28, 2nd-mp = 11 (**b3**) 1st-mp = 22, 2nd-mp = 10

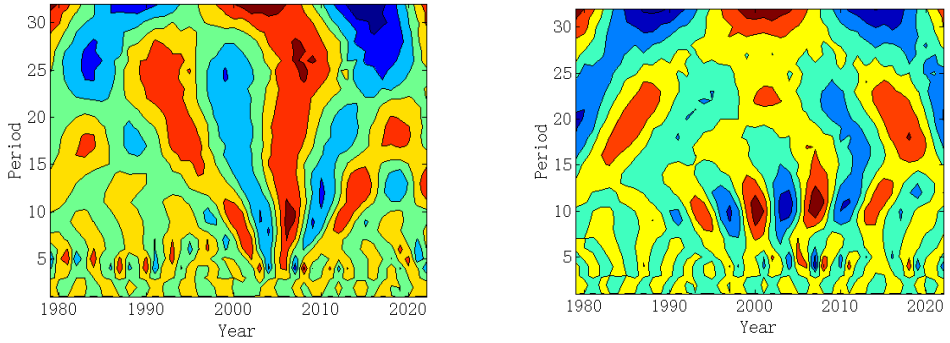

(**a4**) 1st-mp = 26, 2nd-mp = 4 (**b4**) 1st-mp = 10, 2nd-mp = 22

Figure 9. Different time scale wavelet coefficient result graph of upper reach extreme precipitation indices time series. (**a**) upper reach; (**b**) lower reach; (1–4) PRCPTOT, R99p, RX1day, and RX5day.

The number of alternant changes of dryness and abundance of the extreme precipitation indices time series increased, with the time scale decreasing, while the continuity was weakened. By identifying the time scale corresponding to the wavelet variance with the highest energy, we determined that the principal period of the PRCPTOT in the upper

reach was 5a; the principal period of the RX5day in the lower reach was 10a; the principal period of the PRCPTOT, R99p, and RX1day in the lower reach was 22a; the principal period of the RX5day in the upper reach was 26a; and the principal period of the R99p and RX1day in the upper reach was 28a. On the time scale of the first principal period, the alternation process of abundance and dryness was clearer and more complete, and had a global character, especially for the extreme indicators of the lower reach. As a result, most extreme precipitation indices had obvious periodicity on a large time scale, and the extreme precipitation indices of the lower reach had a relatively consistent periodicity, at 22a.

According to the periodicity law, it can be inferred that, in the next few years, the PRCPTOT and RX1day of the upper reach as well as the PRCPTOT, R99p, and RX1day of the lower reach will decrease; in contrast, the R99p and RX5day of the upper reach and the RX5day of the lower reach will increase.

5. Prediction of Extreme Precipitation

The hidden relationship of historical precipitation and forecasted precipitation was clarified based on historical data by using a BP-ANN, thereby predicting the extreme precipitation indices in 2023. This study provided references to water resource management in 2023, consequently facilitating flood prevention and drought relief. The forecasted results exhibited statistical trends, that is, the probability of extreme precipitation at a specific level was proportional to the point density (Figure 10).

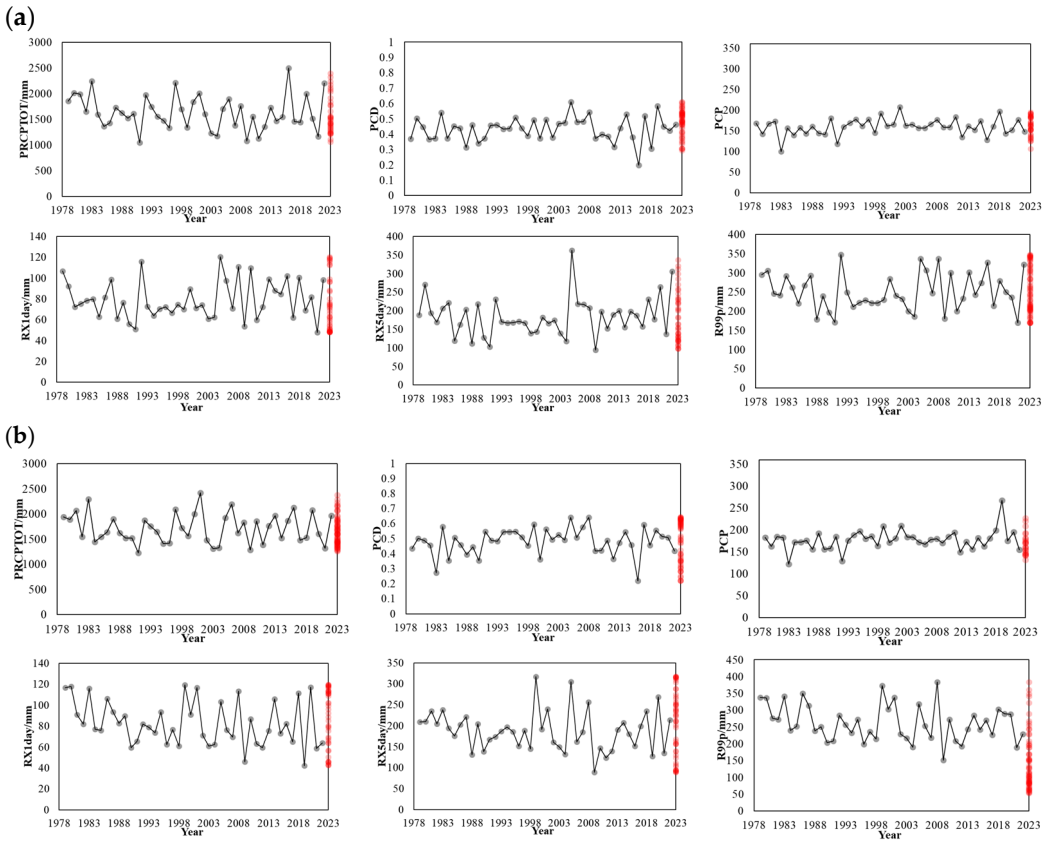

Figure 10. Prediction of annual extreme precipitation indices in 2023: (**a**) upper reach, (**b**) lower reach.

The upper reach was expected to experience lower values of the PRCPTOT, RX1day, and RX5day than the multi-year mean. Hence, it was predicted that the annual precipitation, daily maximum precipitation, and seasonal precipitation of the upper reach in 2023 would be lower than those of normal years. Conversely, the probability of the PCD and PCP being greater than the multi-year mean was high. Hence, we predicted that the PCP would be after June, and the PCD would be higher. The frequencies of occurrences of the predicted

value of the R99p in each case was basically equal. The predicted trends of the PRCPTOT and RX1day were consistent with periodic characteristics, while the predicted trends of the PRCPTOT, PCD and PCP were consistent with changing trends of decades.

For the lower reach, the probability of the PRCPTOT, PCP, and R99p being less than the multi-year mean was high. Thus, we predicted that, in 2023, the annual precipitation and the daily precipitation of the lower reach above the 99th percentile would decrease compared with normal years; the PCP would be before July; and the probability of the PCD, RX1day, and RX5day being greater than the multi-year mean was high. The predicted trends of the PRCPTOT, R99p, and RX5day were consistent with periodic characteristics, while the predicted trends of the PRCPTOT, R99p, PCD, and PCP were consistent with changing trends of decades.

Overall, the total amount of extreme precipitation in 2023 will be less, and the precipitation processes will be more concentrated. Indeed, the upper and lower reaches exhibited opposite extreme precipitation levels, that is, the former was lesser while the latter was greater than normal years.

The qualification rate of extreme precipitation forecasting by the BP-ANN model was 27~72%, mainly 27~36% (Figure 11). The upper reach exhibited slightly poor performance, especially in terms of the PRCPTOT and PCP, when the extreme precipitation index was continuously forecasted based on data correlation; extreme precipitation forecasting in the lower reach was superior to that in the upper reach. Additionally, the qualification rate of R99p prediction reached 72%.

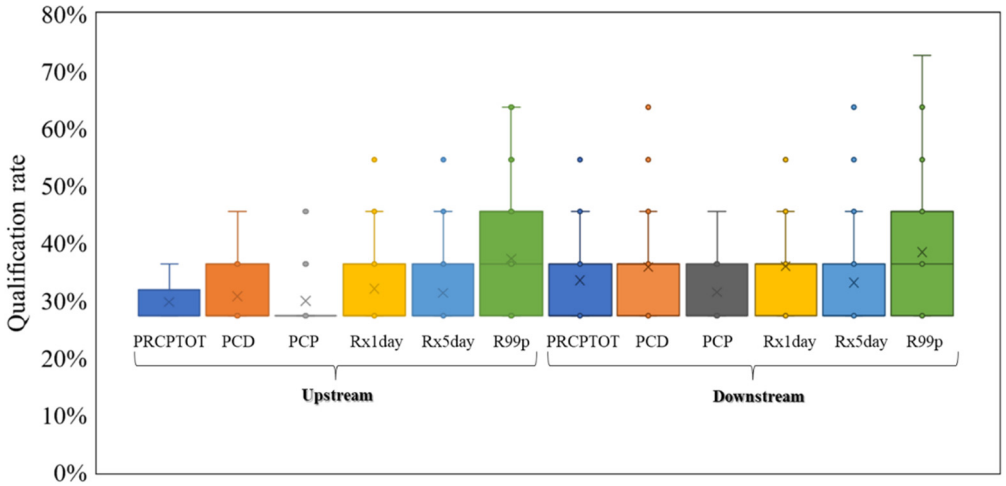

Figure 11. Qualification rate of extreme precipitation forecasting in 2023.

6. Discussion and Conclusions

The spatio-temporal trends of extreme precipitation indices in the target area were evaluated from various perspectives. A BP-ANN model was used to effectively predict the extreme precipitation indices. During the period of 1979–2022, the precipitation of the Dongjiang River Basin underwent significant changes, especially with the increase in extreme climate events in recent years. (1) The topographic features of the Dongjiang River Basin are complex, with active economic activities in the middle reach, lower reach, and estuary delta areas. Owing to geographical location and climate change, there were obvious differences in the precipitation process between the upper and lower reaches of the Dongjiang River Basin. The lower reach had a higher PCD and a PCP that was half a month later than in the upper reach, while the extreme precipitation level increased from northeast to southwest. (2) In the past 44 years, there have been tendencies for the PCP to be delayed, the PCD to increase, the total precipitation to decrease, and the extreme precipitation in the upper reach to increase, while it has decreased in the lower reach. Most extreme precipitation indices had obvious periodicity above the large time scale (22a). (3) According to the periodicity law, it can be inferred that the PRCPTOT and RX1day would be less in

the next few years. As the precipitation of the sessions increased, we predicted that the total extreme precipitation would be reduced in 2023, the precipitation process would be more concentrated, the extreme value of the upper reach would be smaller, and that of the lower reach would be larger. However, the extreme performance of the lower reach was stronger than that of the upper reach. Hence, it is necessary to focus on flood control measures in the lower reach while simultaneously strengthening the intensive management of water resources.

The annual precipitation is mostly concentrated in the rainy season, which causes the Dongjiang River Basin to be in a severe drought state for most of the year, and so it can be prone to extreme floods. Therefore, it is necessary to comprehensively and promptly grasp the spatio-temporal variation of water inflows in the basin to formulate an effective water resource system management strategy, and it is meaningful to optimize the spatio-temporal allocation of water resources in the Dongjiang River Basin.

In future studies, we will conduct more in-depth research based on seasons and the causes of extreme precipitation. Correspondingly, meteorological factors such as atmospheric circulation indicators will be used as the input of the BP-ANN model, and the selection of the input layer (forecasting factors) will be optimized, so as to provide accurate and effective input for the forecasting models, thereby enhancing the efficiency and effectiveness of extreme precipitation forecasting.

Author Contributions: X.C. and N.L. contributed to discovering problems and proposing research ideas; N.L. and W.L. undertook the work of data collection, programming, data processing, visualization, and drafting; X.C., J.Q. and B.Z. were responsible for supervision, inspection, guidance, and suggestions for revision of the manuscript; X.C. and J.Q. provided funding acquisition. All authors have read and agreed to the published version of the manuscript.

Funding: This study was supported by the National Natural Science Foundation of China (51861125203), the Guangdong–Hong Kong Joint Laboratory for Water Security (2020B1212030005), the Water Resource Science and Technology Innovation Program of Guangdong Province (202201), the Fundamental and Applied Basic Research Fund of Guangdong Province (2022A1515010898), and the Special Fund for the Stable Support for Provincial Scientific Research Institutions (2021L027).

Institutional Review Board Statement: Not applicable.

Informed Consent Statement: Not applicable.

Data Availability Statement: All data used during the study can be acquired from the following website: https://www.noaa.gov/ (accessed on 30 March 2023).

Acknowledgments: We thank the Guangdong Research Institute of Water Resources and Hydropower for providing scientific research environment support.

Conflicts of Interest: The authors declare no conflict of interest.

References

1. Lin, L.; Gao, T.; Luo, M.; Ge, E.; Yang, Y.; Liu, Z.; Zhao, Y.; Ning, G. Contribution of urbanization to the changes in extreme climate events in urban agglomerations across China. *Sci. Total Environ.* **2020**, *744*, 140264. [CrossRef] [PubMed]
2. Guo, S.; Guo, E.; Zhang, Z.; Dong, M.; Wang, X.; Fu, Z.; Guan, K.; Zhang, W.; Zhang, W.; Zhao, J. Impacts of mean climate and extreme climate indices on soybean yield and yield components in northeast China. *Sci. Total Environ.* **2022**, *838*, 156284. [CrossRef] [PubMed]
3. Chen, X.; Wang, L.; Niu, Z.; Zhang, M.; Li, J. The effects of projected climate change and extreme climate on maize and rice in the Yangtze River Basin, China. *Agric. For. Meteorol.* **2020**, *282*, 107867. [CrossRef]
4. Huang, C.C.; Pang, J.; Zha, X.; Su, H.; Jia, Y. Extraordinary floods related to the climatic event at 4200 a bp on the Qishuihe river, middle reaches of the Yellow River, China. *Quat. Sci. Rev.* **2011**, *30*, 460–468. [CrossRef]
5. Yang, L.; Scheffran, J.; Qin, H.; You, Q. Climate-related flood risks and urban responses in the Pearl River Delta, China. *Reg. Environ. Change* **2015**, *15*, 379–391. [CrossRef]
6. Liang, C.; Li, D.; Yuan, Z.; Liao, Y.; Nie, X.; Huang, B.; Wu, X.; Xie, Z. Assessing urban flood and drought risks under climate change, China. *Hydrol Process.* **2019**, *33*, 1349–1361. [CrossRef]
7. Adamowski, K.; Bougadis, J. Detection of trends in annual extreme rainfall. *Hydrol Process.* **2003**, *17*, 3547–3560. [CrossRef]

8. Wilcox, E.M.; Donner, L.J. The frequency of extreme rain events in satellite rain-rate estimates and an atmospheric general circulation model. *J. Clim.* **2007**, *20*, 53–69. [CrossRef]
9. Panthou, G.; Vischel, T.; Lebel, T. Recent trends in the regime of extreme rainfall in the central Sahel. *Int. J. Climatol.* **2014**, *34*, 3998–4006. [CrossRef]
10. Amiri, M.A.; Gocić, M. Analyzing the applicability of some precipitation concentration indices over Serbia. *Theor. Appl. Climatol.* **2021**, *146*, 645–656. [CrossRef]
11. Yeşilırmak, E.; Atatanır, L. Spatiotemporal variability of precipitation concentration in western Turkey. *Nat. Hazards* **2016**, *81*, 687–704. [CrossRef]
12. Zhang, T.; Wang, Y.; Liu, B.; Sun, Y.; Chen, X. Variation of hourly extreme precipitation in the Three Gorges reservoir region, China, from the observation record. *Water* **2021**, *13*, 2855. [CrossRef]
13. Sun, C.; Huang, G.; Fan, Y. Multi-indicator evaluation for extreme precipitation events in the past 60 years over the Loess Plateau. *Water* **2020**, *12*, 193. [CrossRef]
14. Tabari, H. Climate change impact on flood and extreme precipitation increases with water availability. *Sci. Rep.* **2020**, *10*, 1–10. [CrossRef] [PubMed]
15. Mann, H.B. Nonparametric tests against trend. *Econom. J. Econom. Soc.* **1945**, *13*, 245–259. [CrossRef]
16. Kendall, M.G. Rank Correlation Methods. In *Charles Griffin*; A Charles Griffin Book: London, UK, 1975.
17. Lazoglou, G.; Anagnostopoulou, C.; Tolika, K.; Kolyva-Machera, F. A review of statistical methods to analyze extreme precipitation and temperature events in the Mediterranean region. *Theor. Appl. Climatol.* **2019**, *136*, 99–117. [CrossRef]
18. Grotjahn, R.; Black, R.; Leung, R.; Wehner, M.F.; Barlow, M.; Bosilovich, M.; Gershunov, A.; Gutowski, W.J.; Gyakum, J.R.; Katz, R.W.; et al. North American extreme precipitation events and related large-scale meteorological patterns: A review of statistical methods, dynamics, modeling, and trends. *Clim. Dyn.* **2019**, *53*, 6835–6875.
19. Ansa Thasneem, S.; Chithra, N.; Thampi, S.G. Analysis of extreme precipitation and its variability under climate change in a river basin. *Nat. Hazards* **2019**, *98*, 1169–1190. [CrossRef]
20. Xu, D.; Liu, D.; Yan, Z.; Ren, S.; Xu, Q. Spatiotemporal variation characteristics of precipitation in the Huaihe River Basin, China, as a result of climate change. *Water* **2023**, *15*, 181. [CrossRef]
21. Bodri, L.; Čermák, V. Prediction of extreme precipitation using a neural network: Application to summer flood occurrence in Moravia. *Adv. Eng. Softw.* **2000**, *31*, 311–321. [CrossRef]
22. André de Sousa Araújo, A.; Silva, A.R.; Zárate, L.E. Extreme precipitation prediction based on neural network model–A case study for southeastern Brazil. *J. Hydrol.* **2022**, *606*, 127454. [CrossRef]
23. Vandal, T.; Kodra, E.; Ganguly, A.R. Intercomparison of machine learning methods for statistical downscaling: The case of daily and extreme precipitation. *Theor. Appl. Climatol.* **2019**, *137*, 557–570. [CrossRef]
24. He, Y.; Lin, K.; Chen, X. Effect of land use and climate change on runoff in the Dongjiang River Basin of south China. *Math. Probl. Eng.* **2013**, *2013*, 471429. [CrossRef]
25. Ding, J.; Jiang, Y.; Fu, L.; Liu, Q.; Peng, Q.; Kang, M. Impacts of land use on surface water quality in a subtropical river basin: A case study of the Dongjiang River Basin, southeastern China. *Water* **2015**, *7*, 4427–4445. [CrossRef]
26. Chen, C.; Yu, Z.; Li, L.; Yang, C. Adaptability evaluation of trmm satellite rainfall and its application in the dongjiang river basin. *Procedia Environ. Sci.* **2011**, *10*, 396–402. [CrossRef]
27. Yang, L.E.; Chan, F.K.S.; Scheffran, J. Climate change, water management and stakeholder analysis in the Dongjiang River Basin in south China. *Int. J. Water Resour. Dev.* **2018**, *34*, 166–191. [CrossRef]
28. Jie, X.; Yu, X.; Na, L.; Hao, W. Spatial and temporal patterns of supply and demand balance of water supply services in the Dongjiang Lake Basin and its beneficiary areas. *J. Resour. Ecol.* **2015**, *6*, 386–396. [CrossRef]
29. Ho, K.; Chow, Y.; Yau, J. Chemical and microbiological qualities of the east river (Dongjiang) water, with particular reference to drinking water supply in Hong Kong. *Chemosphere* **2003**, *52*, 1441–1450. [CrossRef]
30. Li, J.; Chen, Q.W.; Li, D.M. Study on water resources compensation characteristics of dongjiang river basin based on set pair analysis. In Proceedings of the 2011 International Conference on Computer Distributed Control and Intelligent Environmental Monitoring, Changsha, China, 19–20 February 2011.
31. Karl, T.R.; Nicholls, N.; Ghazi, A. Clivar/GCOS/WMO Workshop on Indices and Indicators for Climate Extremes Workshop Summary. In *Weather and Climate Extremes: Changes, Variations and a Perspective from the Insurance Industry*; Karl, T.R., Nicholls, N., Ghazi, A., Eds.; Springer: Dordrecht, The Netherlands, 1999; pp. 3–7.
32. Maghrebi, M.; Noori, R.; Mehr, A.D.; Lak, R.; Darougheh, F.; Razmgir, R.; Farnoush, H.; Taherpour, H.; Moghaddam, S.M.R.A.; Araghi, A.; et al. Spatiotemporal changes in Iranian rivers' discharge. *Elem. Sci. Anthr.* **2023**, *11*, 00002. [CrossRef]
33. Noori, R.; Woolway, R.I.; Saari, M.; Pulkkanen, M.; Kløve, B. Six decades of thermal change in a pristine lake situated north of the Arctic Circle. *Water Resour. Res.* **2022**, *58*, e2021WR031543. [CrossRef]
34. Gdeisat, M.A.; Abid, A.; Burton, D.R.; Lalor, M.J.; Lilley, F.; Moore, C.; Qudeisat, M. Spatial and temporal carrier fringe pattern demodulation using the one-dimensional continuous wavelet transform: Recent progress, challenges, and suggested developments. *Opt. Lasers Eng.* **2009**, *47*, 1348–1361. [CrossRef]
35. Rumelhart, D.E.; Hinton, G.E.; Williams, R.J. Learning representations by back-propagating errors. *Nature* **1986**, *323*, 533–536. [CrossRef]

36. Noori, R.; Karbassi, A.R.; Mehdizadeh, H.; Vesali-Naseh, M.; Sabahi, M.S. A framework development for predicting the longitudinal dispersion coefficient in natural streams using an artificial neural network. *Environ. Prog. Sustain. Energy* **2011**, *30*, 439–449. [CrossRef]
37. Zhang, Q.; Gu, X.; Li, J.; Shi, P.; Singh, V.P. The impact of tropical cyclones on extreme precipitation over coastal and inland areas of China and its association to ENSO. *J. Clim.* **2018**, *31*, 1865–1880. [CrossRef]